СООБЩЕНИЯ
ОБЪЕДИНЕННОГО
ИНСТИТУТА
ЯДЕРНЫХ
ИССЛЕДОВАНИЙ
Дубна

E1 - 5349

Z.S. Strugalski, I. .V. Chuvilo, T. Gemesy,
I.A. Ivanovskaya, Z. Jablonski, T. Kanarek,
S. Krasnovsky, L.S. Okhrimenko,
G. Pinter, B. Słowinski

STUDY OF THE EFFECTIVE MASS SPECTRA OF THE $\gamma\gamma$, $\pi^0\gamma$, $\pi^0\gamma\gamma$, $\pi^0\pi^0$, $\pi^0\eta^0$, $\pi^0\pi^0\gamma$, $\pi^0\pi^0\pi^0$ SYSTEMS IN THE MASS VALUE REGION M $(\gamma \ldots\ldots \gamma) \leq 1.3$ GeV

1970

E1 - 5349

Z.S. Strugalski, I. .V. Chuvilo, T. Gemesy,
I.A. Ivanovskaya, Z. Jablonski, T. Kanarek,
S. Krasnovsky, L.S. Okhrimenko,
G. Pinter, B. Słowinski

STUDY OF THE EFFECTIVE MASS SPECTRA OF THE $\gamma\gamma$, $\pi^0\gamma$, $\pi^0\gamma\gamma$, $\pi^0\pi^0$, $\pi^0\eta^0$, $\pi^0\pi^0\gamma$, $\pi^0\pi^0\pi^0$ SYSTEMS IN THE MASS VALUE REGION M $(\gamma \ldots\ldots \gamma) \leq 1.3$ GeV

1. Introduction

In film obtained in an exposure of the JINR 550 x 280 x 160 mm^3 xenon bubble chamber to a 2.34 GeV/c π^+ beam, we have searched for production and decays of neutral bosons decaying into π^0 mesons and gamma-quanta. This experiment uses over 500000 stereophotographs of the chamber.

There are many physical topics concerning such decays of bosons. These are connected, for example, with the problems of the existence of new neutral mesons/1/, with the examination of the consequences of SU_6 theory/2/, and with the verification of the possible C , T noninvariance in the electromagnetic interactions of strongly interacting particles/3-5/. It is important also to obtain the complete set of information concerning the neutral decays of η^0- , ω^0 - , and X^0 -mesons.

We present in this paper the experimental results which can be attributed to some of the above mentioned problems. The distributions of effective mass: $M(\gamma\gamma)$, $M(\pi^0\gamma)$, $M(\pi^0\gamma\gamma)$, $M(\pi^0\pi^0)$, $M(\pi^0\pi^0\gamma)$, $M(\pi^0\pi^0\pi^0)$ from γ ..... γ combinations are given. The general features of the experimental results and the methodical problems, especially the problems of background, were considered.

2. Experimental Procedure

The scanning for interactions of beam particles occuring in a chosen central region of the bubble chamber (fig. 1) has been made twice in succession. The interactions with 1 and 2 prongs and with some number $k = 0, 1, 2, \ldots$ of gamma-quanta ascribed to these interactions are searched.

Confining oneself to the investigation of the interactions with one observed secondary track stopping within the chamber, we can assume the selected interactions to be in general the processes/6-8/

$$\pi^+ + n \rightarrow \underset{\hookrightarrow k\,\gamma}{X} + p \quad , \tag{1}$$

n being quasi-free neutron in Xenon nucleus; X denotes any particle decaying into π^0's and gamma-quanta. The energy of the secondary charged particle, assumed to be proton, can be estimated by means of the range-energy relation. It is possible to select in this way the reactions of the type (1) in which total energy of secondaries, gamma-quanta and proton, is equal to the energy of incoming π^+ mesons. Then, the possibility exists to investigate the particles with the effective mass values $M(\gamma \ldots \gamma) \leq 1300$ MeV. It is worth to note that our results do not depend on the fact being the interactions of the type (1) on the quasi-free nucleons or not.

The minimum energy value for detectable protons in stars with a small number of prongs (less than 4) is about 5 MeV. π^+ mesons can be identified by means of the observation of the charged decay products: $\pi^+ \rightarrow \mu^+ \rightarrow e^+$, and π^- mesons with energies higher than 10 MeV can be distinguished from protons. The lower limit of energy for gamma-quanta detectable in the chamber with nearly constant efficiency is about 15 MeV.

For each event the coordinates of the interaction points and of the gamma-quanta conversion points were measured with the accuracy $\Delta X = \Delta Y = 0.1$ mm, $\Delta Z = 0.5$ mm, as well as the total track length of electrons and positrons in gamma-quanta initiated showers. The accuracy of measurement of the angles $\Theta_{\gamma\gamma}$ between any two gamma-quanta emission directions is equal to $(0.5 - 2)^{\circ}$. Using the special scanning tables the total track lengths of shower particles were measured many times by different scanners. From these data the energies of gamma-quanta E_γ were estimated according to the method worked out /9-12/. During the track lengths measurements additional control of gamma-quanta numbers in events analysed, and the fulfilling of scanning criteria were proved. The optimal energy measurement accuracy equals 12%. Those events were analysed only in which the gamma-quanta energy measurement accuracy was no worse than 35%.

With due regard for the statistical weights of gamma-quanta we can perform good estimation of the number of events belonding to some class of reactions. The recording probability of gamma-quanta generated in chosen central region of the chamber and recorded within the fiducial volume, and that for which the energy can be estimated with an accuracy $\Delta E_\gamma / E_\gamma \leq 35\%$ makes up 80-95% being in dependence from the number of gamma-quanta in event. Average observation probability for all gamma-quanta equals 94%.

Thus, having the information about gamma-quanta energy E_γ, and about gamma-quanta emission angles Θ_γ for each event it is possible to estimate invariant mass $M(k\gamma)$ combining some number k of gammas. It was found that k can be equal up to 8 and it is still possible to distinguish single gamma-quanta and to evaluate E_γ. The gamma-quanta used for estimation of $M(k\gamma)$ are observed as generated in the point of interaction of incident meson. Thus, the mass $M(k\gamma)$ can be expressed by the formula

For each event the coordinates of the interaction points and of the gamma-quanta conversion points were measured with the accuracy $\Delta X = \Delta Y = 0.1$ mm, $\Delta Z = 0.5$ mm, as well as the total track length of electrons and positrons in gamma-quanta initiated showers. The accuracy of measurement of the angles $\Theta_{\gamma\gamma}$ between any two gamma-quanta emission directions is equal to $(0.5 - 2)^{\circ}$. Using the special scanning tables the total track lengths of shower particles were measured many times by different scanners. From these data the energies of gamma-quanta E_γ were estimated according to the method worked out /9-12/. During the track lengths measurements additional control of gamma-quanta numbers in events analysed, and the fulfilling of scanning criteria were proved. The optimal energy measurement accuracy equals 12%. Those events were analysed only in which the gamma-quanta energy measurement accuracy was no worse than 35%.

With due regard for the statistical weights of gamma-quanta we can perform good estimation of the number of events belonding to some class of reactions. The recording probability of gamma-quanta generated in chosen central region of the chamber and recorded within the fiducial volume, and that for which the energy can be estimated with an accuracy $\Delta E_\gamma / E_\gamma \leq 35\%$ makes up 80-95% being in dependence from the number of gamma-quanta in event. Average observation probability for all gamma-quanta equals 94%.

Thus, having the information about gamma-quanta energy E_γ, and about gamma-quanta emission angles Θ_γ for each event it is possible to estimate invariant mass $M(k\gamma)$ combining some number k of gammas. It was found that k can be equal up to 8 and it is still possible to distinguish single gamma-quanta and to evaluate E_γ. The gamma-quanta used for estimation of $M(k\gamma)$ are observed as generated in the point of interaction of incident meson. Thus, the mass $M(k\gamma)$ can be expressed by the formula

$$M^2(k\gamma) = \sum_{\substack{i\,j=1 \\ i\neq j}}^{n} M^2(\gamma_i\ \gamma_j) \qquad (2)$$

$$M^2(\gamma_i\,\gamma_j) = 2E_{\gamma_i} E_{\gamma_j} (1 - \cos\Theta_{\gamma_i\ \gamma_j})$$

irrespectively whether the gamma-quanta are generated independently by the radiative decay of some particle X or by decays of X via, for example, π^0 - or η^0 -mesons. The accuracy of $M(k\gamma)$ determination depends on the energy estimation accuracy and on the accuracy of the opening angle between two gamma-quanta. For events with $k = 2$ the optimal accuracy reaches, in average, 10-12%, for events with $k = 3$ - about 8-10%, and for events with $k = 4$ - about 7-8%. The average accuracy of $M(k\gamma)$ determination makes up 15-20%.

3. Experimental Data

Out of 500000 photographs about 2000 events of the type (1) were selected. For 1362 events the energies of gamma-quanta could be measured with the given accuracy. Later on only those events will be analysed in detail. Table 1 presents the distribution of events according to the numbers of gamma-quanta.

Table 1

Distribution of events of the type (1) according to the number of gamma-quanta

Type of event	Number of events recorded	
	observed	evaluated
$k = 2$	746	1052
$k = 3$	230	441
$k = 4$	306	657
$k = 5$	29	70
$k = 6$	51	126

The events containing observable V^0 particles are not placed in Table 1. About 160 events with one and about 50 events with two V^0 were found.

3.1. General Information

a) Search for possible influence of the geometry of the chamber on results obtained.

The location within the chamber of the region chosen for interactions being under consideration is shown in fig. 1.

The distribution of azimuthal angles of emission of gamma-quanta φ was done with purpose to examine the correctness of the gamma-quanta efficiency evaluation/13/ (fig. 2). Thus, taking into account the gamma-quanta efficiency, the true number of events is well estimated irrespectively of the numbers of gammas in events under cosideration.

b) Kinetical energies of charged secondaries.

Kinetical energies E_{kp} of charged secondaries in the reactions of the type (1), assuming the secondaries to be protons, were obtained from the relation range-energy with the accuracy of about 5%.

The distribution of protons according E_{kp} is shown in fig. 3 for events with any number of gamma-quanta. In fig. 4 the distribution of events according to the total energies of secondaries, $\Sigma E_\gamma + E_{kp}$, is presented.

c) Energy and angular distributions of gamma-quanta.

The energy spectra of gamma-quanta in events with any number of gammas are shown in fig. 5. The distributions of emission angles of gamma-quanta are presented in fig. 6.

d) The statistical independence of gamma-quanta recorded.

Gamma-quanta are emitted, on the whole, via decay of some particles into π^0 s and gammas. As regards this some reason exists to suppose the statistical dependence of gamma-quanta recor-

ded may display. It is obvious that apriori one cannot state: Is the estimation of recording probability of event with k gamma-quanta well performed, assuming the gammas to be statistical independent, or not?

In order to estimate the said dependence, the average probabilities of registration of events with k gamma-quanta were evaluated using the formulas:

$$\overline{P_k^m} = \frac{\sum_{i=1}^{n} (P_k^m)_i}{n} \qquad (3)$$

and

$$\overline{P_k^{m'}} = \prod_{i=1}^{m} (\overline{P_k^1})_i \quad . \qquad (4)$$

$\overline{P_k^m}$ and $\overline{P_k^{m'}}$ - the average recording probabilities of m gamma-quanta in events with k gamma-quanta; the number of m gamma-quanta combinations is lettered by n . P_k^1 - average recording probability of one gamma-quantum in events with k gamma-quanta; P_k^m - probability of registration of m gamma-quanta in events with k gamma-quanta. The results are presented in Table 2.

It is evident from this analysis the statistical dependence of gamma-quanta does not practically become apparent in events considered.

3.2. Two Gamma-Quanta Events

We have plotted in fig. 7 the distribution of the effective mass $M_{2\gamma}$. The significant peak at the π^0 meson mass value is observed, as it must. The second group is observed in the region of the η^0 meson mass value. The shaded part of histogram represents background from the events with k more than 2. Solid line -

Table 2

Data for examination of the statistical independence of gamma-quanta

k	$\gamma \ldots \gamma$ combination	m					
		1	2	3	4	5	6
2	$\overline{P^m_k}$	0.87	0.72				
	$\overline{P^{m'}_k}$	-	0.73				
6	$\overline{P^m_k}$	0.86	0.76	0.64	0.56	0.48	0.40
	$\overline{P^{m'}_k}$	-	0.74	0.63	0.54	0.47	0.40

the Gaussian distribution with σ = 120 MeV normalized to the number of events in mass value interval 400-700 MeV.

The distribution of the opening angle $\Theta_{\gamma\gamma}$ of gamma-quanta emission directions in the laboratory system is shown in fig. 8. In this histogram two groups of events are also observed. A first being in the region of minimum value of the $\Theta^{min}_{\gamma\gamma}$ for π^0 meson, and the second one at minimum value of $\Theta_{\gamma\gamma}$ for η^0 meson. The distributions of the events in these two groups are in good agreement with the theoretical distribution for π^0 mesons (curve 1) and for η^0 mesons (curve 2).

3.3. Three Gamma- Quanta Events

Fig. 9 shows the spectrum of the effective mass $M_{3\gamma}$ of the three gamma-quanta events. The solid curve is the background obtained by the Monte-Carlo method and normalized to the total number of events. For evaluation of this curve the experimental angular and energy spectra of gamma-quanta from the events under consideration were used.

The histigram in fig. 10 represents the spectrum of the effective mass $M^{2\gamma}_{3\gamma}$ of two gamma-quanta system in the three gamma-quanta events, and shows a significant peak at the π^0 meson mass value. The solid curve is evaluated by the Monte-Carlo method and normalized to the total number of events with $M^{2\gamma}_{3\gamma}$ mass values equal or less than 90 MeV.

3.4. Four Gamma-Quanta Events

For 306 events we have evaluated the effective mass of four gamma-quanta systems, $M_{4\gamma}$. Fig. 11 shows the mass spectra obtained after taking into account the gamma-quanta recording probability. The solid curve represents the phase space for reaction $\pi^+ + n \to \pi^0 + \pi^0 + p$ at 2.34 GeV/c π^+ meson momentum.

The spectrum of effective mass of two gamma-quanta system in the sample of four gamma-quanta events is shown in fig. 12. The smooth curve, the random gamma gamma combination distribution, was calculated using the Monte-Carlo method and was normalized to the total number of events with mass values $M^{2\gamma}_{4\gamma}$ equal or less than 90 MeV. In this histogram a significant peak at M_{π^0} value stands well out against a background.

The sample of four gamma-quanta events was divided into three groups: 1. the events in which the two independent gamma-gamma combinations, from all the six possible, give the values of $M^{2\gamma}_{4\gamma}$ lying within the mass value interval prescribed for π^0 -mesons; 2. the events in which only one gamma-gamma combination gives the $M^{2\gamma}_{4\gamma}$ value prescribed for π^0 meson and the other independent gamma-gamma combination do not form the $M^{2\gamma}_{4\gamma}$ prescribed for π^0 mesons; 3. the events in which one of gamma-gamma combinations gives the mass value $M^{2\gamma}_{4\gamma}$ prescribed for π^0 mesons and the other independent gamma-gamma combination gives the value of $M^{2\gamma}_{4\gamma}$ which can be ascribed to the η^0 meson. The mass value interval 90-180 MeV was accepted as permissible for π^0 meson mass values, and the mass value interval 400-700 MeV was accepted as permissible for η^0 meson mass values, in agreement with the

mass estimation accuracy of about 30%. The notations $M(\pi^0\pi^0)$, $M(\pi^0\gamma\gamma)$ and $M(\pi^0\eta^0)$ will be used in the course of this paper for effective mass $M_{4\gamma}$ in these three groups of events.

Fig. 13 shows the distribution of $M(\pi^0\pi^0)$ after substraction of the background from six gamma-quanta events. The dotted line histogram represents the distribution of random $\pi^0 - \pi^0$ combinations normalized to the number of events with mass value of $M(\pi^0\pi^0)$ less than 500 MeV.

In Fig. 14 the mass distribution of $M(\pi^0\gamma\gamma)$ is shown. Solid curve representing the background is normalized to the total number of events with mass values $M(\pi^0\gamma\gamma)$ less than 400 MeV.

Distribution of effective mass $M(\pi^0\eta^0)$ in the sample of events of the third group is shown in fig. 15. The effective mass distribution $M^{3\gamma}_{4\gamma}$ in the samples of $\pi^0\pi^0$, $\pi^0\gamma\gamma$, and $\pi^0\eta^0$ events are shown in fig. 16. Normalization is performed to the same number of events.

3.5. Five Gamma - Quanta Events

Distribution of effective mass $M_{5\gamma}$ is presented in fig. 17. The distribution of effective mass $M^{5\gamma}_{6\gamma}$ of five gamma-quanta combinations for six gamma-quanta events is also there presented. Normalization has been performed to the number of events with mass values $M_{5\gamma}$ less than 700 MeV. The analysis shows existence of only the $\pi^0\pi^0\gamma$ type of events, except one in all sample being under consideration. This is also very easy to see from the distribution of gamma-gamma effective mass $M^{2\gamma}_{5\gamma}$ which is shown in fig. 18. By means of the solid curve the background normalized to the total number of events with mass values below 90 MeV is presented.

The distribution of $M^{4\gamma}_{5\gamma}$: $M^{4\gamma}_{5\gamma}(\pi^0\pi^0)$ and $M^{4\gamma}_{5\gamma}(\pi^0\gamma\gamma)$ are shown in fig. 19 and in fig. 20. In figs. 21 and 22 the distributions $M^{3\gamma}_{5\gamma}(\gamma\gamma\gamma)$ and $M^{3\gamma}_{5\gamma}(\pi^0\gamma)$ are shown.

3.6. Six Gamma - Quanta Events

The effective mass spectrum of six gamma-quanta combinations for six gamma-quanta events is shown in fig. 23. The curve 1 represents the η^0 meson effective mass distribution taking into account the mass estimation errors. Normalization is performed in the mass values interval of $M_{6\gamma}$ less than 550 MeV. The curve 2 is the phase space for non resonant three π^0's production. In all events, except one, presence of three π^0 mesons is established. It is easy to see it also from the $M^{2\gamma}_{6\gamma}$ distribution presented in fig. 24. Background is normalized to the number of events with the values of effective mass of gamma-gamma combinations being equal or less than 90 MeV.

The distributions of $M^{5\gamma}_{6\gamma}(\pi^0\pi^0\gamma)$, $M^{4\gamma}_{6\gamma}(\pi^0\pi^0)$, $M^{4\gamma}_{6\gamma}(\pi^0\gamma\gamma)$ are shown in figs. 25, 26, and 27. In fig. 28 the distributions of $M^{3\gamma}_{6\gamma}(\pi^0\gamma)$ and $M^{3\gamma}_{6\gamma}(\gamma\gamma\gamma)$ are given.

4. Results and Discussion

Let us sum up briefly the main results following from the survey of histograms presented above.

1. The analysis of $M^{2\gamma}_{k\gamma}$ distributions in any sample of k gamma-quanta events of the type (1), with $k = 2$-6, shows the existence of a significant peak at the π^0 meson mass value. The number of π^0 mesons observed in any $M^{2\gamma}_{k\gamma}$ distribution is equal always to the number of π^0 mesons expected, which can be ascribed to the corresponding reaction (1). This result shows strong evidence for correctness of our method and indicates the possibility of direct study of particles decaying into π^0 mesons and gamma-quanta.

2. The two gamma-quanta events with mass values $M_{2\gamma}$ within the interval 400-700 MeV in the $M_{2\gamma}$ distribution (fig. 7) can be attributed to the generation of η^0. The other events with mass values in the interval 90-180 MeV can be ascribed to production

of π^0 mesons. In average, the ratio $R_{\eta \to 2\gamma}$ of the number of η^0, to the number of π^0 mesons generated in the reaction of the type (1) is equal to

$$R_{\frac{\eta \to 2\gamma}{\pi^0}} = (24.2 \pm 2.7)\% \quad . \tag{5}$$

3. In our sample of events with two gamma-quanta we have not indications about existence of other intensive sources decaying into two gamma-quanta, without π^0 mesons and η^0 mesons.

4. Among the events with four gamma-quanta the three groups of events have been selected: $\pi^0\pi^0$, $\pi^0\gamma\gamma$, and $\pi^0\eta^0$.

5. In the effective mass distribution for the sample of four gamma-quanta events with two π^0 mesons a group of events lying above background distribution is easy to see in the mass values region 600-900 MeV. The average value of the $M(\pi^0\pi^0)$ at this region is equal $M(\pi^0\pi^0) = 730 \pm 30$ MeV.

6. In the distribution of $M(\pi^0\gamma\gamma)$ effective mass for four gamma-quanta events the maximum of the number of events at the region of mass values 500-600 MeV is located, being above the background level.

7. It is easy to see the existence of events above the background level at 700-900 MeV in the distributions of effective mass $M_{3\gamma}$ and $M_{5\gamma}$.

The detailed analysis of the experimental results has been also performed. Namely, the spectrum of effective mass of the $\pi^0\pi^0$ system has been studied/14-15/ and the neutral modes of η^0 meson and ω^0 meson decays have been investigated/16-17/. The more complete information concerning those investigations has been presented in our recent papers/14-17/, here the summary of the final results is given only.

A. Effective Mass Spectrum of the $\pi^0-\pi^0$ System

In the $\pi^0-\pi^0$ combinations effective mass distribution, after substraction of the contamination of the wrong events from the reactions with three π^0 mesons in final state, two groups of events lying above background level are observed: one at region of $M(\pi^0\pi^0)$ values 600-900 MeV, and the second one at 1000-1300MeV. Supposing the peaks observed being caused by some resonant $\pi^0-\pi^0$ systems, the Breit-Wigner analysis of $M(\pi^0\pi^0)$ distribution gives the following values for the effective mass:

$$\overline{M}_1(\pi^0\pi^0) = 730 \pm 30 \text{ MeV},$$
$$\overline{M}_2(\pi^0\pi^0) = 1250 \pm 30 \text{ MeV}, \tag{6}$$

and for the widths of the peaks:

$$\Gamma_1 = 170 \pm 87 \text{ MeV},$$
$$\Gamma_2 = 282 \pm 174 \text{ MeV}. \tag{7}$$

The group of events from the mass values interval 1000 - 1300 MeV can be ascribed to the f^0 particle decaying into two π^0 mesons. The other group, at 600-900 MeV can be connected with the famous problem of the dipion system at $M(\pi^0\pi^0)$ value about 700 MeV.

If we suppose the last peak to be caused by some $\pi^0-\pi^0$ resonant system, then we estimate the relative intensity of generation of this system to be

$$\frac{N(\pi^0-\pi^0)}{N(\eta^0\to 2\gamma)} = 0.25 \pm 0.08, \tag{8}$$

using information about the intensity of $\eta^0\to 2\gamma$ production in our experiment.

B. Neutral Decay Modes of the η^0 Particle

Using results of the analysis of the two gamma-quanta, four gamma-quanta, and six gamma-quanta events and performing the accurate analysis of the corresponding distribution we have estimated the following η^0 meson branching ratios/17/:

$$\frac{N(\eta^0 \to 2\gamma)}{N(\eta^0 \to \text{neutrals})} = (57 + 9)\% \ .$$

$$\frac{N(\eta^0 \to \pi^0\gamma\gamma)}{N(\eta^0 \to \text{neutrals})} = (11 \pm 3)\% \ , \qquad (9)$$

$$\frac{N(\eta^0 \to \pi^0\pi^0\pi^0)}{N(\eta^0 \to \text{neutrals})} = (32 \pm 9)\% \ .$$

C. Neutral Decay Modes of the ω^0 Particle

In the distribution of effective mass $M_{3\gamma}$ for the sample of three gamma-quanta events some indications for existence of events of the $\omega^0 \to \pi^0\gamma$ and of the $\omega^0 \to \eta^0\gamma \to 3\gamma$ decays can be evident after additional selection of three gamma-quanta events/16/. Namely, these events should be singled out in which the total energy of three gamma-quanta is no less than 700 MeV, and the directions of gamma-quanta emission are lying out the cone with the opening angle values β fulfilling the relation $1/2\ 3 > 0.32$ /16/.

In the sample of five gamma-quanta events some indication for possible existence of five gamma-quanta system with mass value lying near the ω^0 meson mass value can be obtained after substraction of the background from the six gamma-quanta events/16/.

Supposing the observed presence of some number of such three and five gamma-quanta events lying above background level at ω^0 meson mass value region to be caused by the ω^0 meson decays, the following ω^0 meson neutral decay modes branching ratios have beer estimated:

$$\frac{N(\omega^0 \to \eta^0\gamma \to 3\gamma)}{N(\omega^0 \to \pi^0\gamma)} = (22 \pm 8)\ \%\ ,$$

$$\frac{N(\omega^0 \to \pi^0\pi^0\gamma)}{N(\omega^0 \to \pi^0\gamma)} = (16 \pm 13)\ \%\ . \qquad (10)$$

References

1. A.M. Baldin. Nuovo Cimento., 37, 962 (1965).
2. S. Badier and C. Bouchiat. Phys.Letter., 15, 96 (1965).
3. J. Bernstein, G. Feinberg, T.D. Lee. Phys.Rev., 139, B165 (1965).
4. G. Feinberg. Phys.Rev., 140, B1402 (1965).
5. V.I. Sakharov, A.B. Kaidalov. JETP, 50, 203 (1966).
6. Z.S. Strugalski, T. Siemiarczuk. Phys.Lett., 11, 170 (1964).
7. M. Daszkiewicz, B. Slowinski, Z.S. Strugalski. Journ. of Nucl. Phys., 5, 341 (1967).
8. B. Slowinski, Z.S. Strugalski. JINR preprint, P1-3822, Dubna (1968).
9. Z.S. Strugalski. JINR Preprint , 796, Dubna (1961).
10. L.P. Konovalova, L.S. Okhrimenko, Z.S. Strugalski. PTE, 6, 26 (1961).

11. O. Czyzewski, J. Danysz, Z.S. Strugalski. Acta Physica Polonica, 24, 509 (1963).
12. I.A. Ivanovskaya, T. Kanarek, L.S. Okhrimenko, B. Slowinski, Z.S. Strugalski, I.V. Chuvilo, Z. Jablonski. Pribory i Technica Experimenta, 2, 39 (1968).
13. L.S. Okhrimenko, B. Slowinski, Z.S. Strugalski. JINR preprint, P13-3918, Dubna (1968).
14. Z.S. Strugalski, I.V. Chuvilo, I.A. Ivanovskaya, Z. Jablonski, T. Kanarek, L.S. Okhrimenko, T.E. Fenyves, T. Gemesy, S. Krasnovsky, G. Pinter. Phys. Lett., 29B, 518 (1969).
15. Z.S. Strugalski, I.V. Chuvilo, I.Y. Ivanovskaya, Z. Jablonski, T. Kanarek, L.S. Okhrimenko, B. Slowinski, E. Fenyves, T. Gemesy, S. Krasnovsky, G. Pinter. JINR Preprint, E1-5085, Dubna (1968).
16. Z.S. Strugalski, I.V. Chuvilo, I.A. Ivanovskaya, Z. Jablonski, T. Kanarek, L.S. Okhrimenko, E. Fenyves, T. Gemesy, S. Krasnovsky, G. Pinter. Phys.Lett., 29B, 532 (1969).
17. Z.S. Strugalski, I.V. Chuvilo, I.A. Ivanovskaya, Z. Jablonski, T. Kanarek, L.S. Okhrimenko, T. Gemesy, S. Krasnovsky, G. Pinter, JINR preprint, E1-5256, Dubna (1970).

Received by Publishing Department
on August 24, 1970.

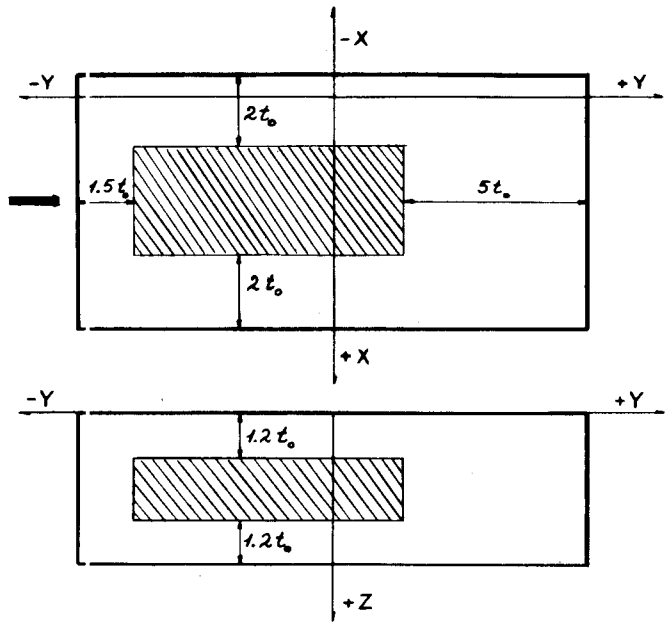

Fig. 1. Location of the chosen region of interactions in the xenon bubble chamber.

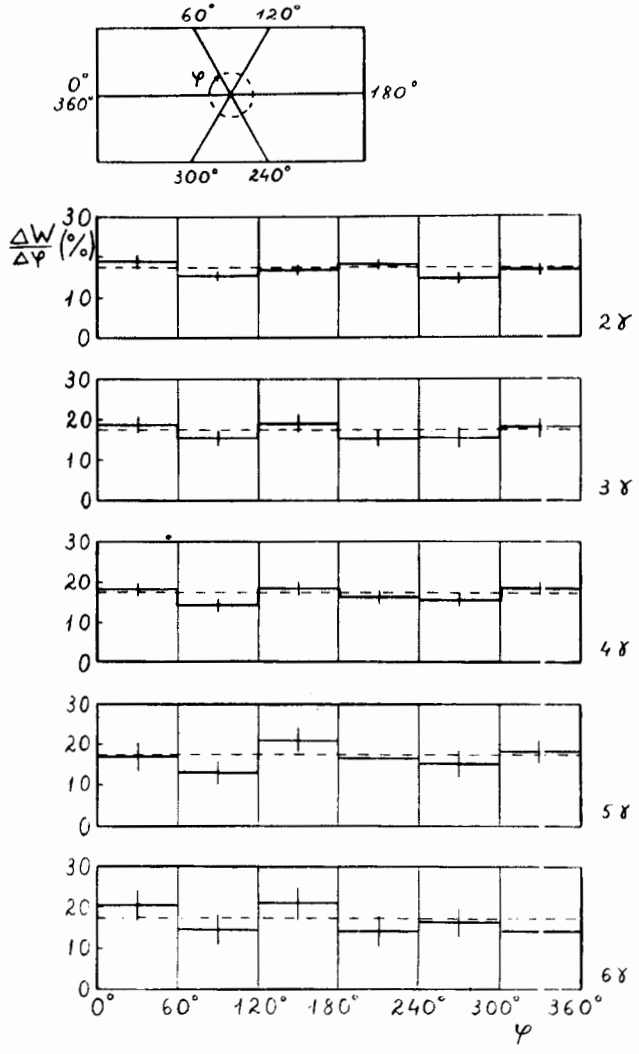

Fig. 2. Distributions of gamma-quanta emission azimuthal angles in events with different k_γ .

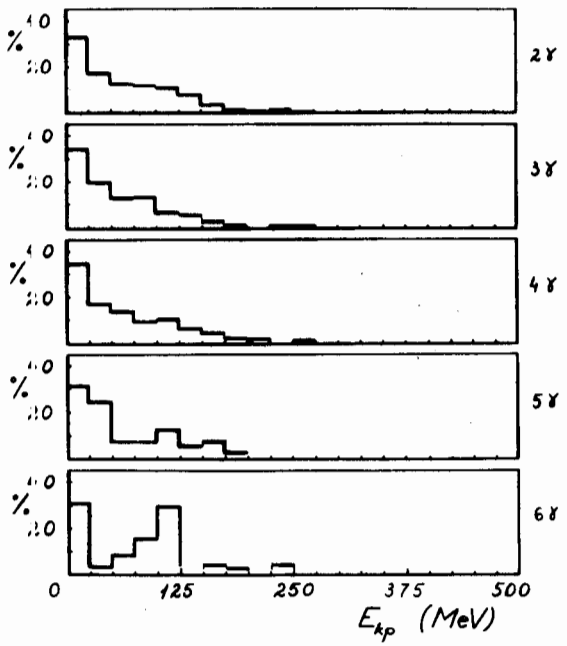

Fig. 3. Energy spectra of protons in reactions (1).

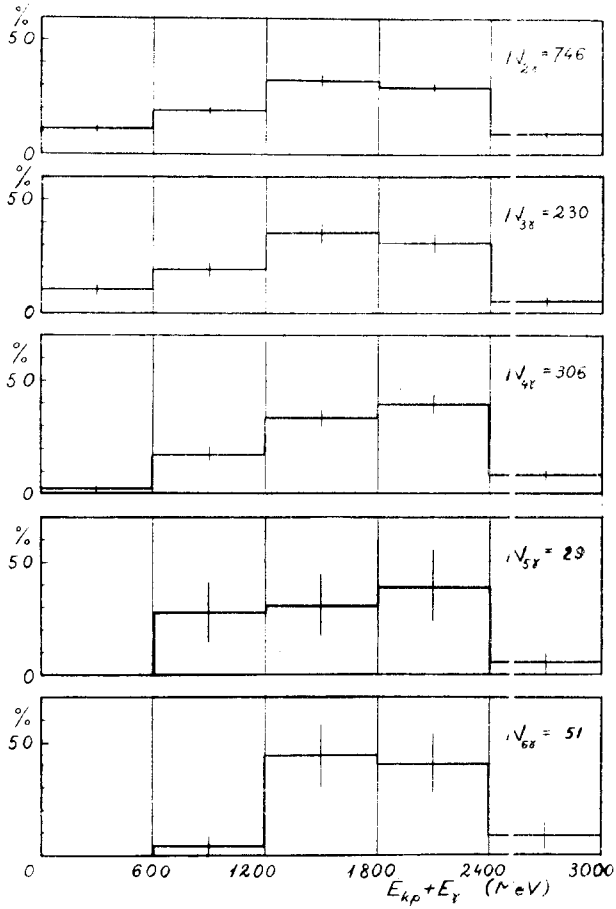

Fig. 4. Distributions of the total energies of secondaries in the events discussed.

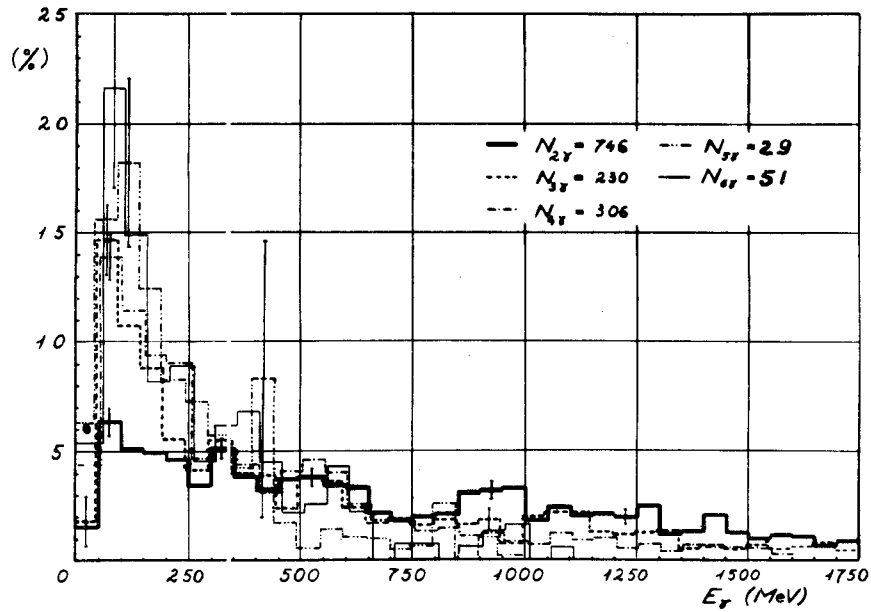

Fig. 5. Energy spectra of gamma-quanta in the events with 2,3, 4, 5 and 6 gamma-quanta.

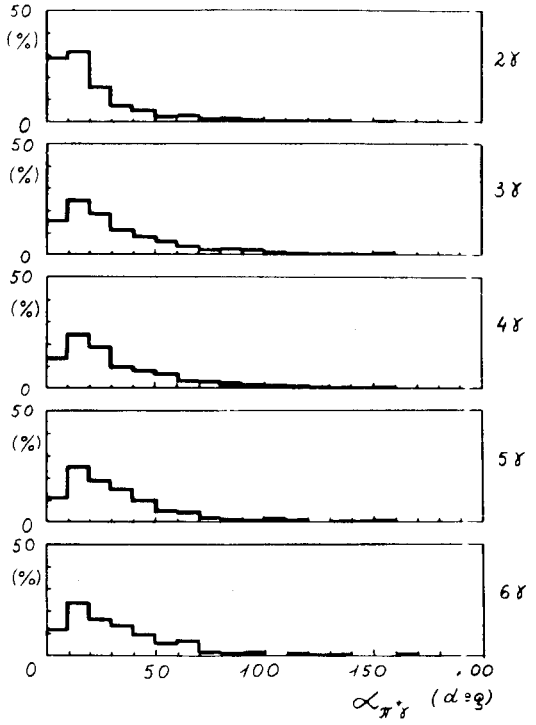

Fig. 6. Gamma-quanta emission angles distribution in events with 2,3,4,5,6 gamma-quanta.

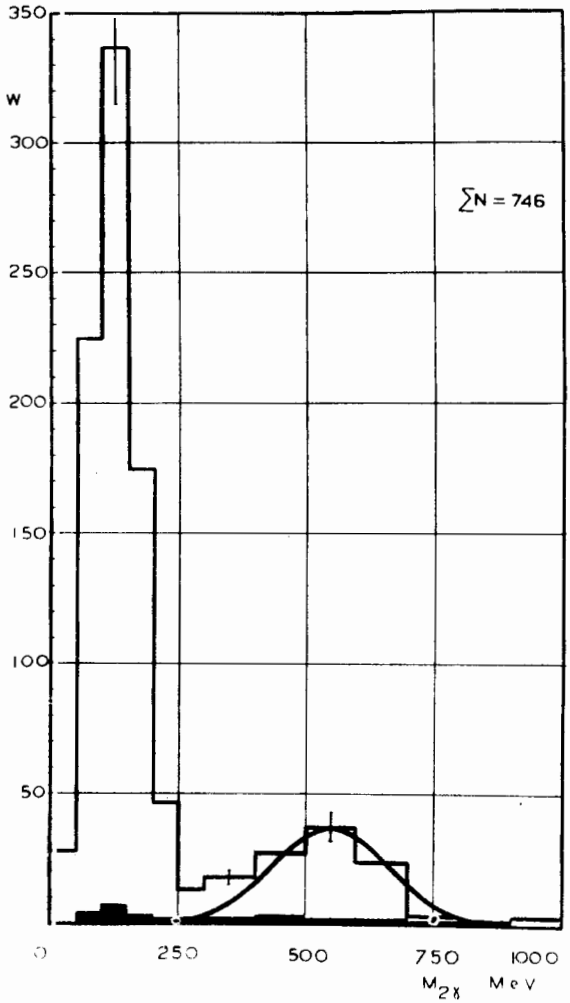

Fig. 7. Distribution of the effective mass $M_{2\gamma}$ in the two gamma-quanta events. The shaded area represemts the back-ground from events with numbers of gamma-quanta more than two. The solid curve shows the Gaussian distribution corresponding to η^0 meson mass measurements accuracy and normalized to the number of events in effective mass value interval 400-700 MeV.

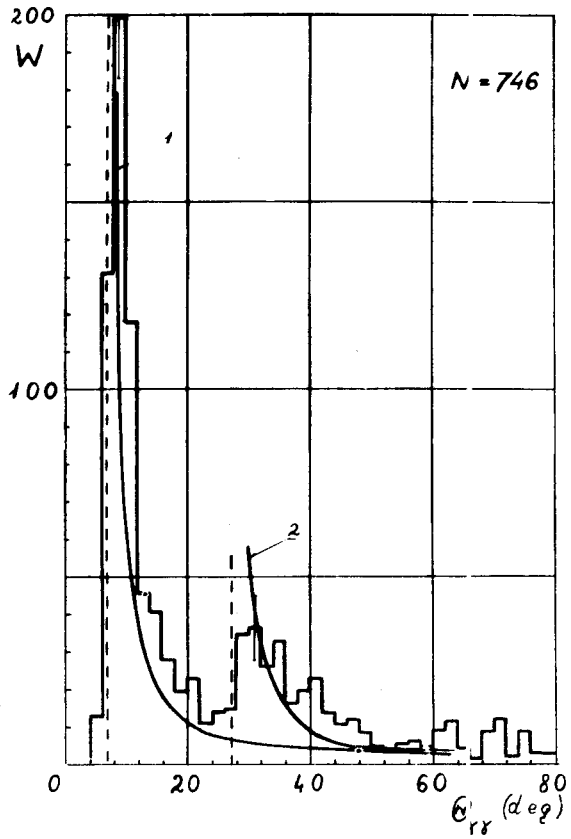

Fig. 8. Distribution of the opening angles $\Theta_{\gamma\gamma}$ of gamma-quanta emission in laboratory system of coordinates for events with two gamma-quanta. The curve 1 - prediction for π^0 mesons, the curve 2 - prediction for η^0 meson.

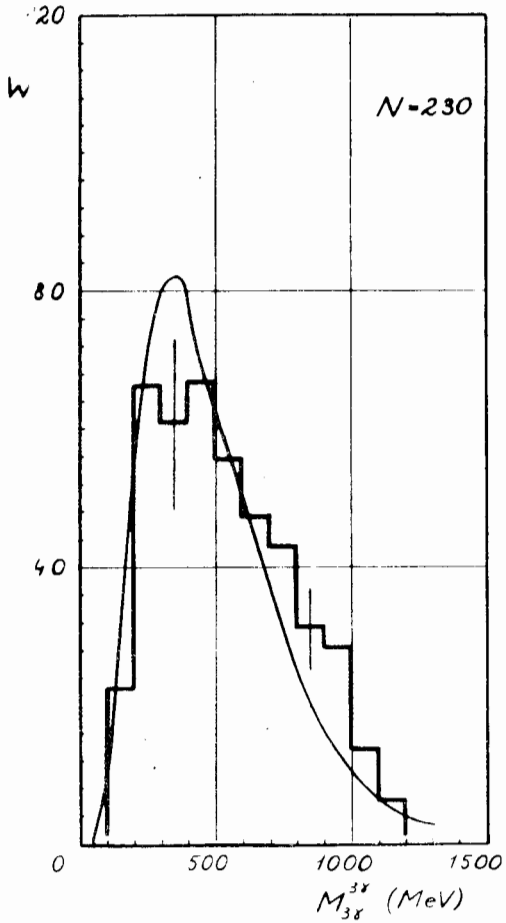

Fig. 9. Distribution of the effective mass $M_{3\gamma}$ for events with three gamma-quanta. The solid curve superimposed on the histogram represents the distribution evaluated by means of Monte-Carlo program. Normalization is performed to the total number of events.

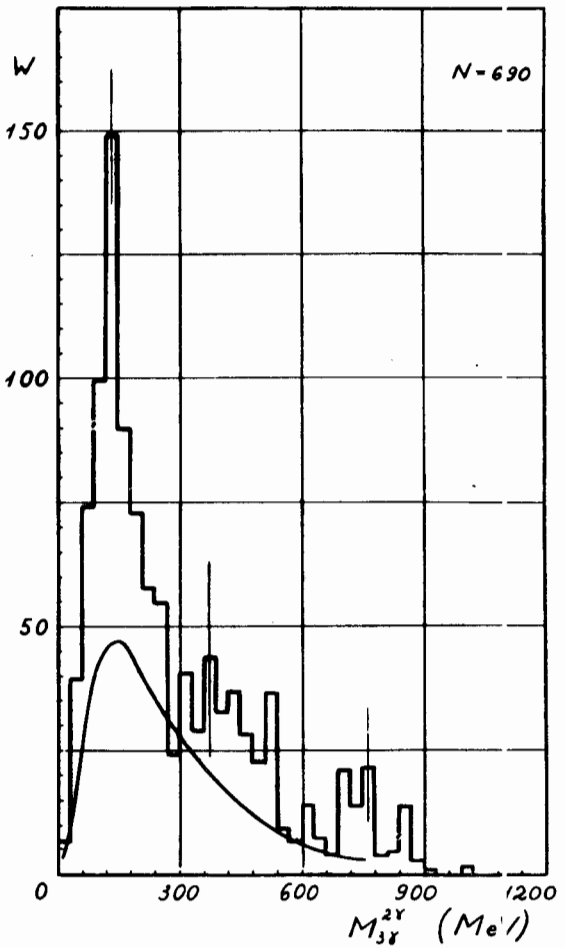

Fig. 10. Distribution of the effective mass $M_{3\gamma}^{2\gamma}$ in events with three gamma-quanta. The solid curve represents the background.

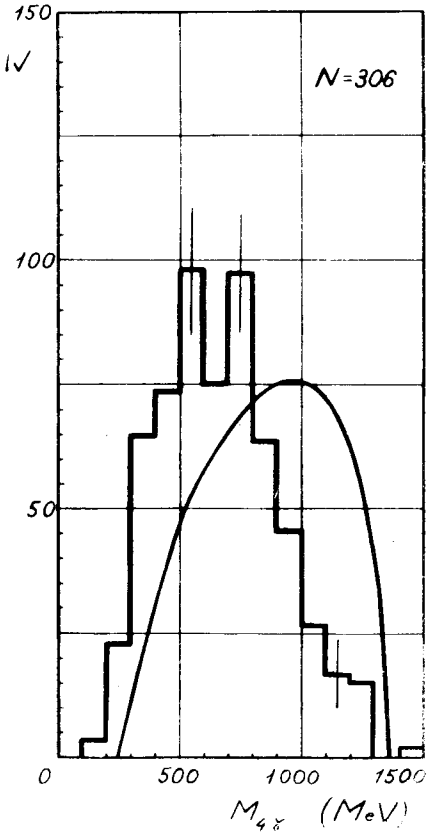

Fig. 11. Distribution of the effective mass $M_{4\gamma}$ in the four gamma-quanta events. The solid curve represents the phase space for reaction $\pi^+ + p \to n + \pi^0$.

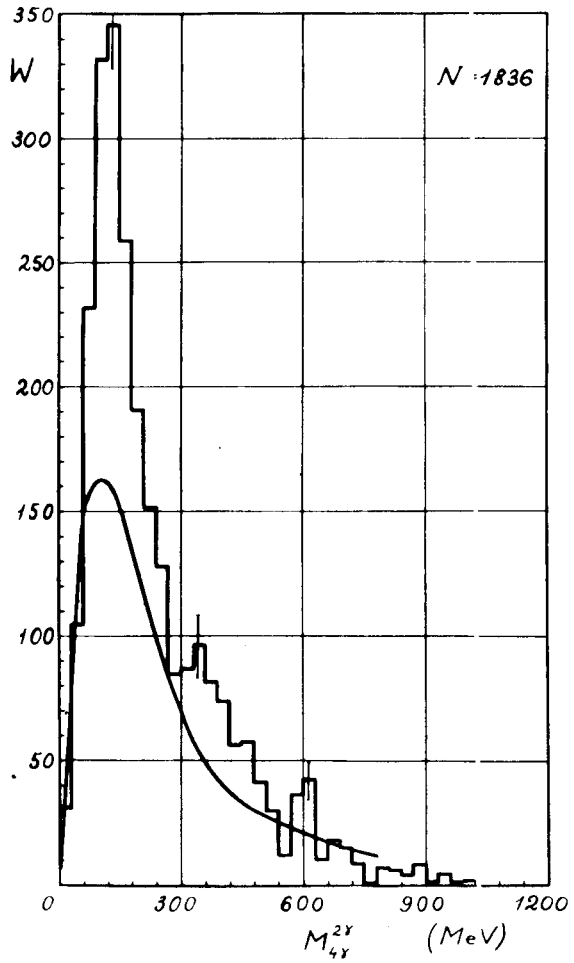

Fig. 12. Distribution of the effective mass $M_{4\gamma}^{2\gamma}$ in the four gamma-quanta events. The solid curve represents background.

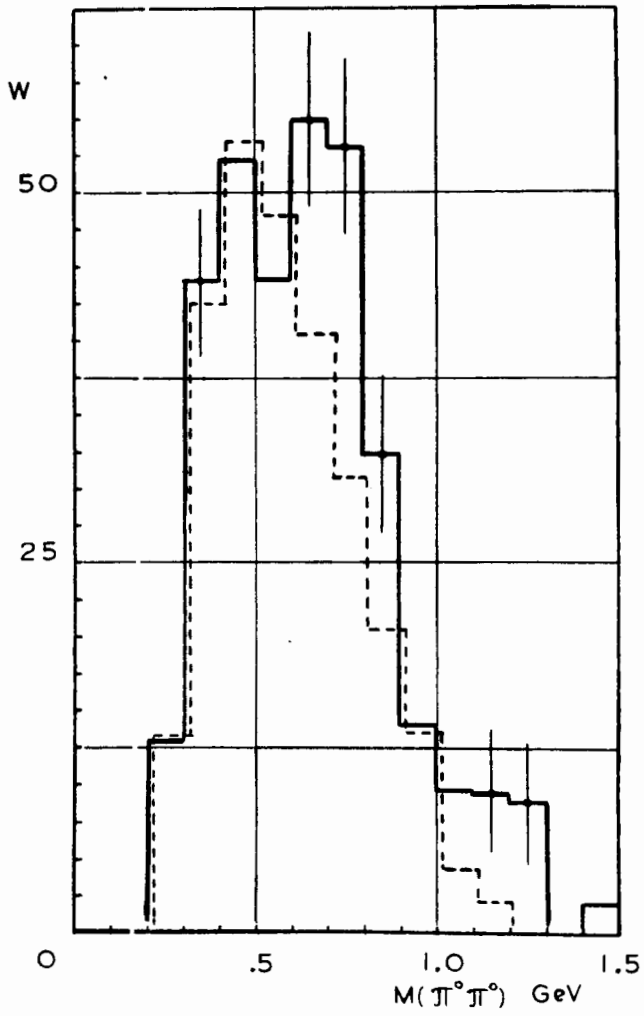

Fig. 13. Distribution of the effective mass $M(\pi^0\pi^0)$ in events with four gamma-quanta. The dotted line histogram represents the random $\pi^0 - \pi^0$ combinations. Normalization is performed to the number of events with mass values equal or less than 500 MeV.

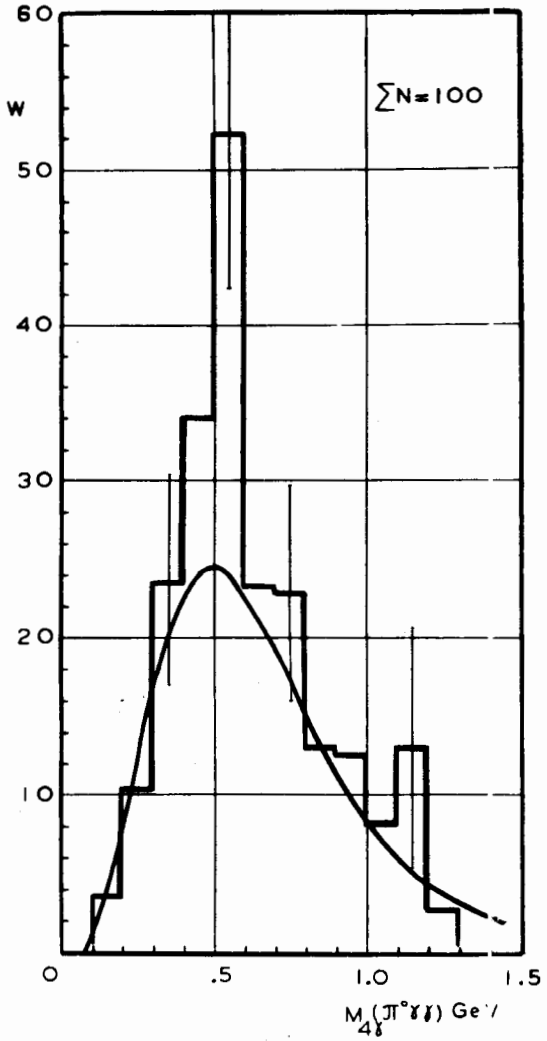

Fig. 14. Distribution of the effective mass $M(\pi^0 \gamma \gamma)$ in the four gamma-quanta events. The solid curve represents he random four gamma-quanta combinations. Normalization is performed to the number of events with mass values equal or less than 400 MeV.

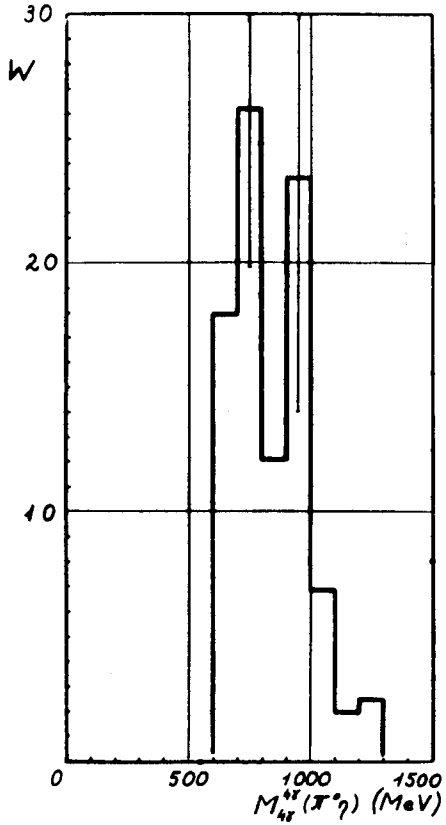

Fig. 15. Distribution of the effective mass $M(\pi^0\eta^0)$ in the four gamma-quanta events.

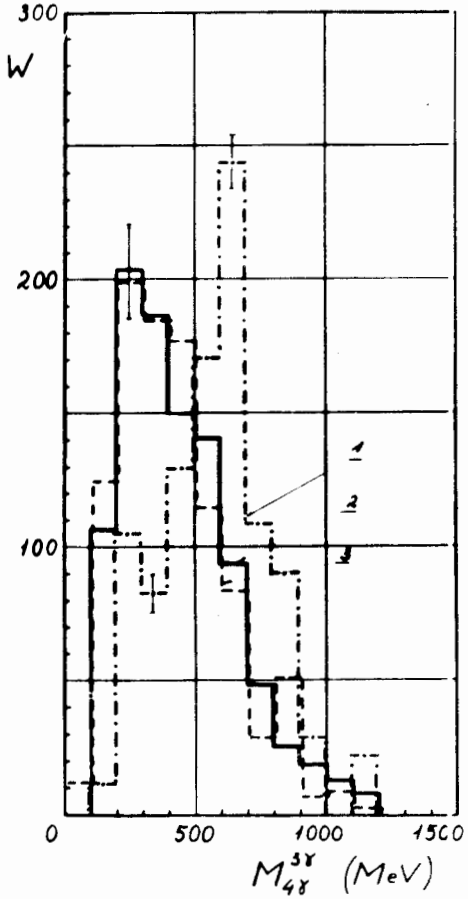

Fig. 16. Distributions of the effective mass $M^{3\gamma}$ in the four gamma-quanta events of the type: 1 - $\pi^0\eta^0$, 2 - $^{4\gamma}\pi^0\pi^0$, 3 - $\pi^0\gamma\gamma$.

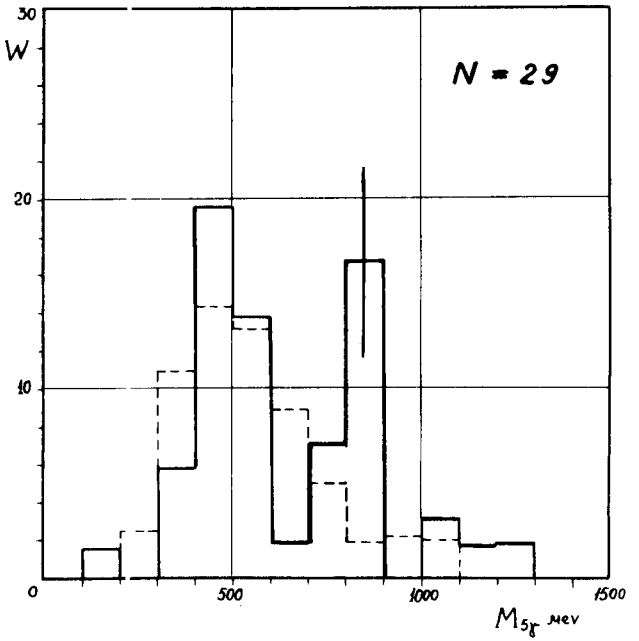

Fig. 17. Distribution of the effective mass $M_{5\gamma}$ in the five gamma-quanta events. The dotted line histogram represents the distribution of $M^{5\gamma}_{6\gamma}$ for six gamma-quanta events. Normalization is performed to the number of events with values of $M_{5\gamma}$ equal or less than 700 MeV.

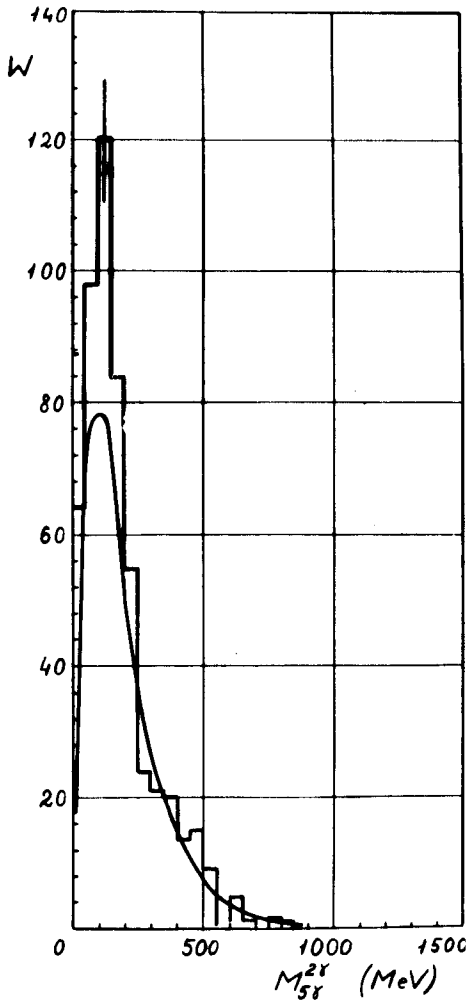

Fig. 18. Distribution of the effective mass $M_{5\gamma}^{2\gamma}$ in the five gamma-quanta events. The solid curve represents backgrounds.

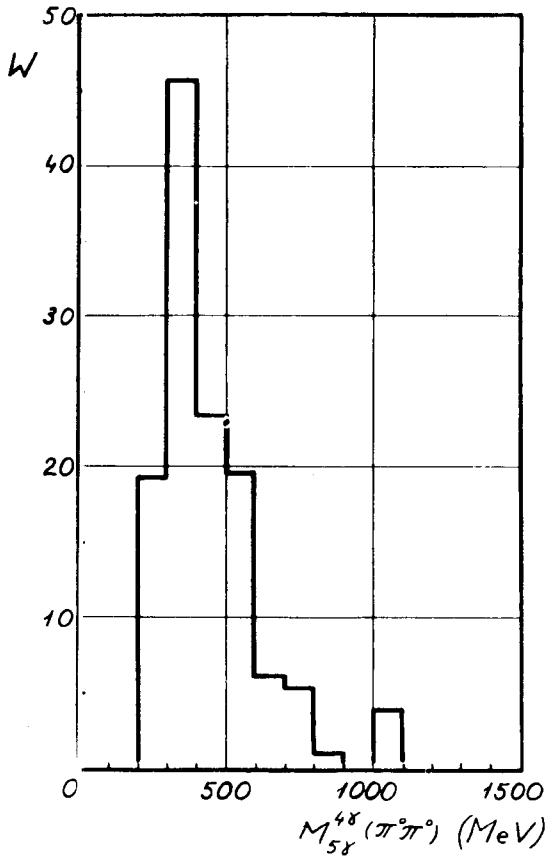

Fig. 19. Distribution of the effective mass $M^{4\gamma}_{5\gamma}(\pi^0\pi^0)$ in events with two π^0 mesons.

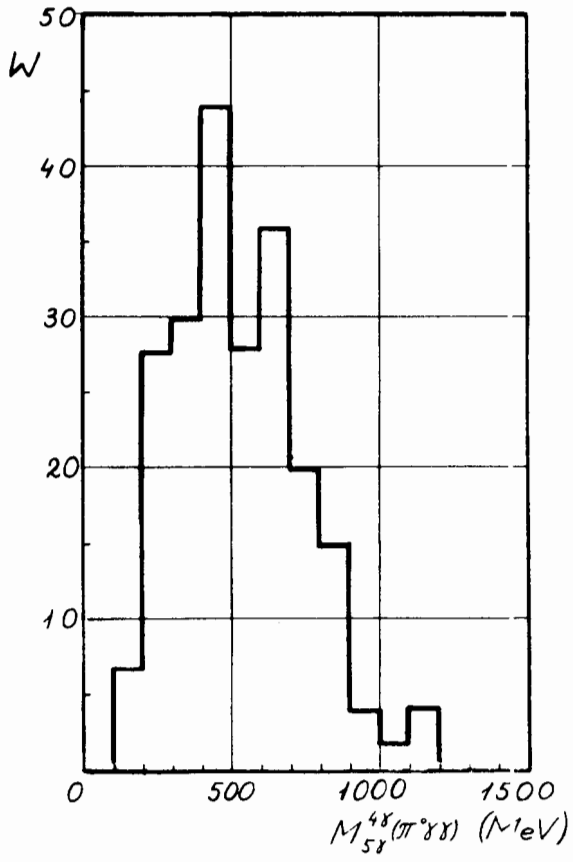

Fig. 20. Distribution of the effective mass $M_{5\gamma}^{4\gamma}(\pi^0\gamma\gamma)$ in the five gamma-quanta events with one π^0 meson.

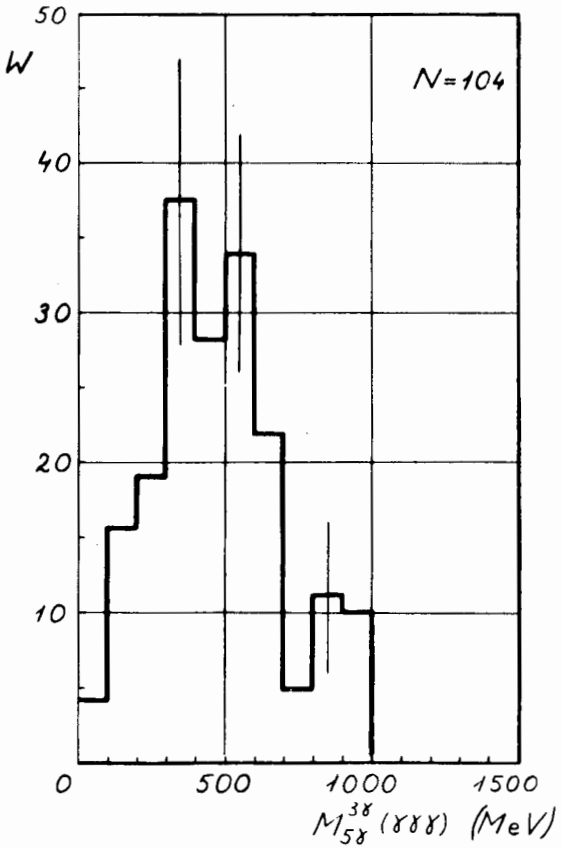

Fig. 21. The distribution of the effective mass $M_{5\gamma}^{3\gamma}(\gamma\gamma\gamma)$.

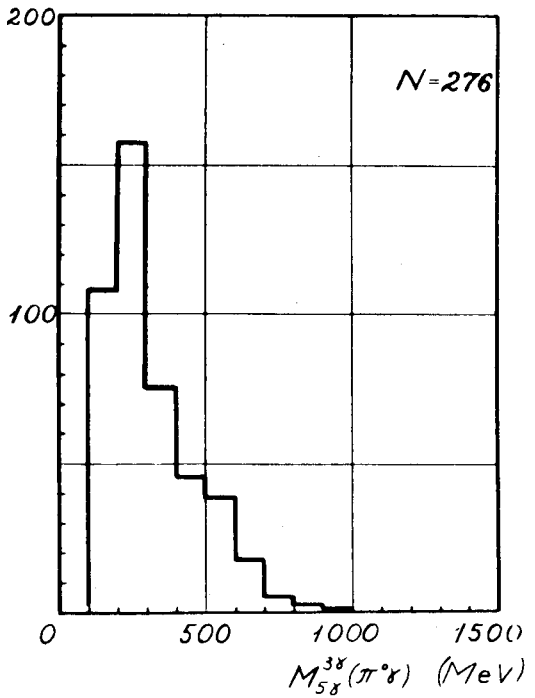

Fig. 22. Distribution of effective mass $M_{5\gamma}^{3\gamma}(\pi^0\gamma)$.

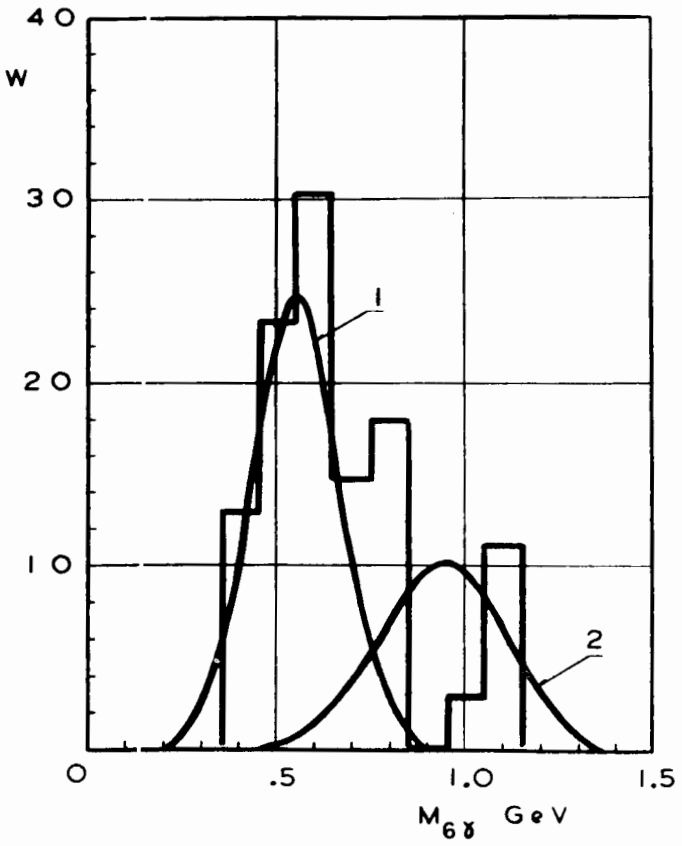

Fig. 23. Distribution of the effective mass $M_{6\gamma}$ in the six gamma-quanta events. The curve 1 represents the Gaussian distribution corresponding to η^0 meson mass measurement accuracy normalized to the number of events with mass values equal or less than 550 MeV. The curve 2 represents the phase space for the reactions of nonresonant production of three π^0 mesons.

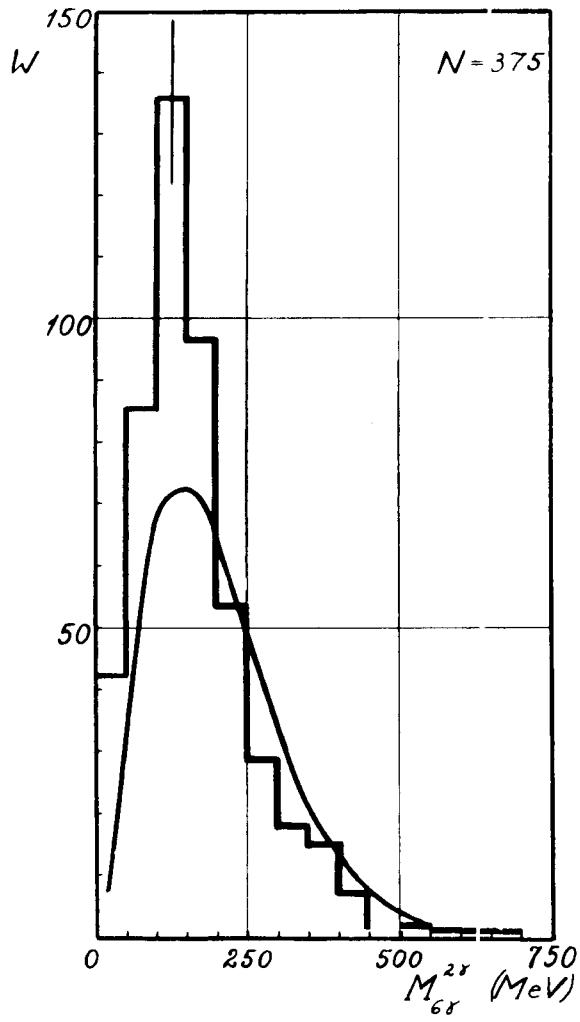

Fig. 24. Distribution of the effective meass $M^{2\gamma}_{6\gamma}$ in the six gamma-quanta events. The solid curve - background.

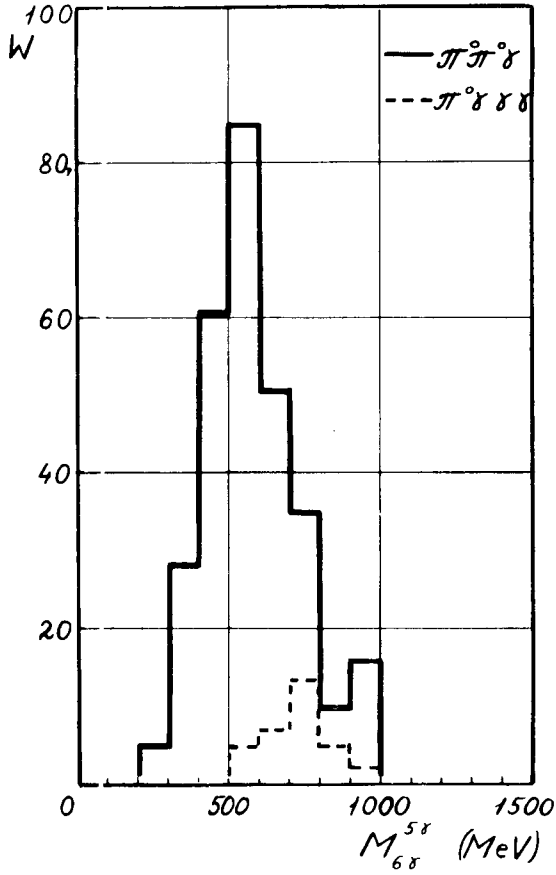

Fig. 25. Distribution of the effective mass $M_{6\gamma}^{5\gamma}(\pi^0\pi^0\gamma)$ in the six gamma-quanta everts.

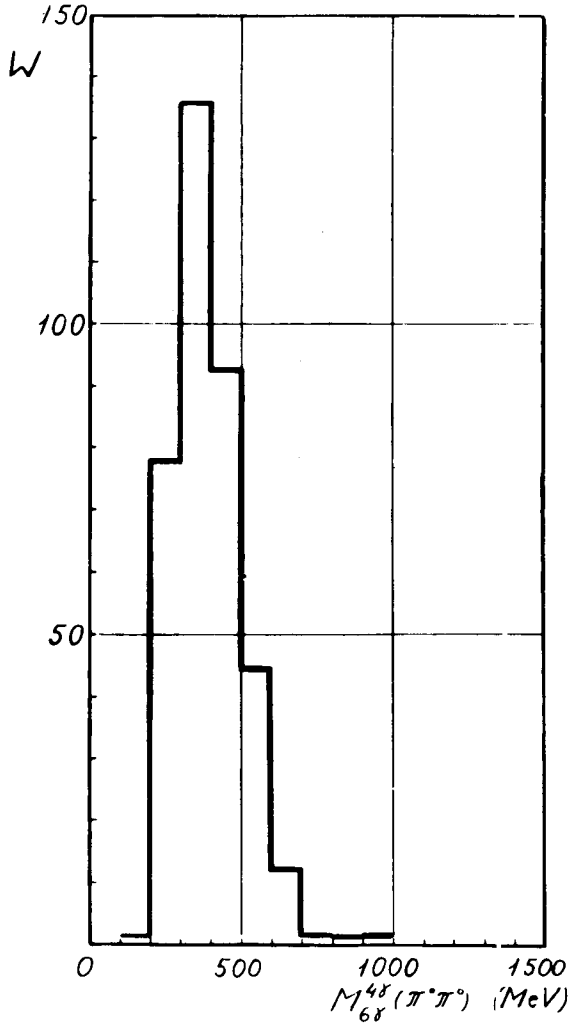

Fig. 26. Distribution of the effective mass $M^{4\gamma}_{6\gamma}(\pi^+\pi^0)$ in the six gamma-quanta events.

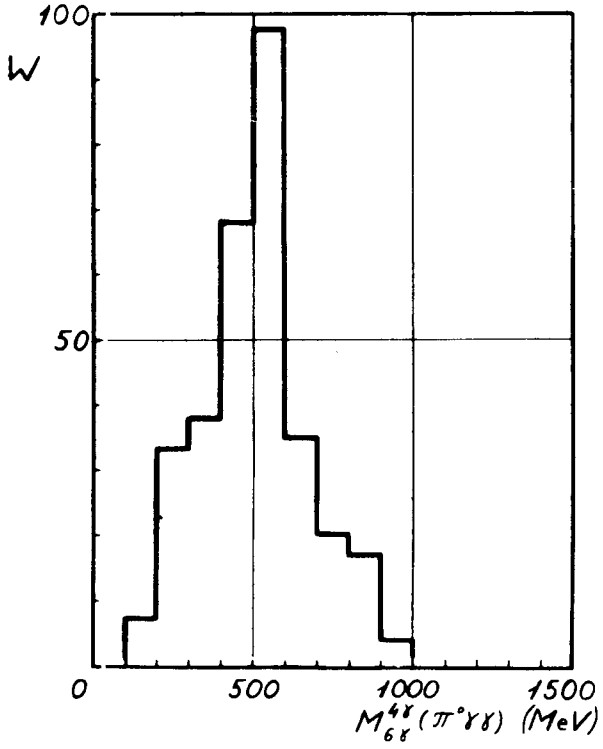

Fig. 27. Distribution of the effective mass $M_{6\gamma}^{4\gamma}(\pi^0\gamma\gamma)$ in the six gamma-quanta events.

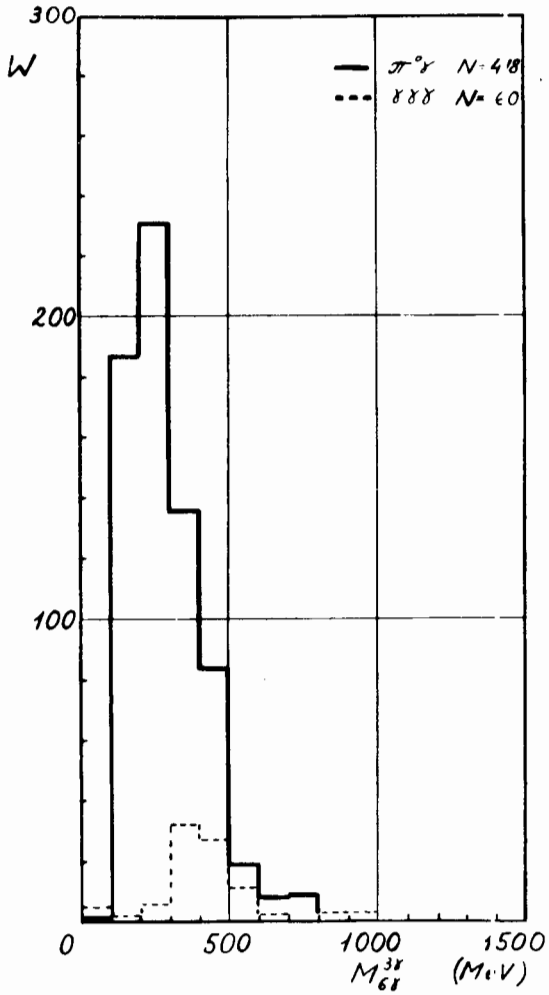

Fig. 28. Distribution of the effective mass $M_{6\gamma}^{3\gamma}(\pi^0\gamma)$ and $M_{6\gamma}^{3\gamma}(\gamma\gamma\gamma)$ in the six gamma-quanta events.